A fluorescence microscopy image showing a field of cells. The cells are mostly dark, but many have bright green spots or patches, indicating the presence of a fluorescent marker. The spots are of varying sizes and are distributed across the field of view. The background is black, making the green spots stand out prominently.

An attempt to elucidate the mechanisms behind the generation of non-canonical peptides through protein electroporation, using the B3Z cellular reporter assay

# Proteasome Catalysed Peptide Splicing

How studying proteasome arts and crafts can increase our understanding of epitope generation

Jacco Bakx

---

## Abstract

The proteasome, through its generation of immunogenic peptides, plays an essential role in the defence against pathogens and tumours. However, recently it has become clear that certain peptides presented on the cell surface have no corresponding sequence in the genome, dubbed non-canonical peptides. As of now, uncertainty of the origin behind these peptides still exists, with theories ranging from translation of (previously thought) untranslated regions of the genome to post-translational RNA modifications. In this research, we will further explore one such theory, called Proteasome Catalysed Peptide Splicing, where the proteasome splices fuses a non-contiguous sequence into a new peptide. To circumvent the usual protein production pathway in which these peptides can arise, we produced protein in *Escherichia coli* and, after thorough purification, were able to successfully introduce it into cells. Subsequently, we inserted a reporter peptide in its contiguous or split form (peptide divided in two using three intervening amino acids) in a *Listeria monocytogenes* derived protein. Through the use of a reporter cell line able to recognize the contiguous version of this peptide, we have been showed that a peptide not originally present in the protein can be found on the cell surface. Based on these results, we conclude this technique is a viable alternative to express proteins intracellularly and that this protein can be processed by the proteasome. Subsequently, we also conclude that non-canonical peptides can be generated from a solely protein-based source.

## Laymen's summary

In order to fight off pathogens and tumours, the body makes a lot of use of little pieces of information called peptides, which can be derived from proteins in a cell. By using the proteasome, a molecular scissor inside the cell, the body can cut up these proteins and present them on a silver platter on the cell surface, also known as the MHC molecules. From there, it can be recognized by immune cells in the body and a fitting reaction can take place, such as the production of antibodies or the killing of tumour cells. This creates a system where there is continuous sampling of the waste products of the cells and allows the body to respond to unknown peptides in a quick and specific matter.

Interestingly, it has been discovered that peptides exist that are not made from simply cutting up existing proteins, called non-canonical peptides. So far it has been unclear what the actual mechanism behind the generation of these peptides is, although possible origins have been proposed. Most theories propose that these peptides are cut from proteins made from faulty blueprints, which normally should not be present.

In this report, one such origin will be explored, the so-called Proteasome Catalysed Peptide Splicing (PCPS). According to this theory, the proteasome does not simply cut all the different proteins, but is also able to paste distant regions of the protein together to create new peptides. To achieve this, we took a protein that was known to produce non-canonical peptides and replaced that part with a widely used reporter peptide (SIINFEKL, derived from egg white proteins), that was either complete or split into two parts (split SIIN/FEKL). These proteins could then be produced inside bacteria and could be purified after, allowing us to use them in further experiments.

Subsequently, we transferred this protein into a cell by giving it electric shocks. After giving the cells time to recover and process the proteins, we then used a reporter cell that could recognize (non-split) SIINFEKL. Afterwards, we could then compare the cells that we gave SIINFEKL-containing proteins, split SIINFEKL-containing proteins or proteins containing neither.

Using this method, we were able to efficiently bring proteins that were produced in bacteria into mammalian cells. Additionally, we saw a presence of non-split SIINFEKL in cells that we only electroporated with split SIINFEKL. From this, we concluded that the proteasome could indeed paste distant parts of proteins together through PCPS.

By modifying parts of the model protein, we can further study the mechanism behind PCPS in future experiments. By better understanding the way in which these non-canonical peptides are produced, we can more accurately predict in the future which peptides can be generated from a given protein. In turn, this will allow us to make better vaccines against pathogens and even tumour cells.

## Table of contents

Abstract .....	1
Laymen’s summary.....	2
Acknowledgements .....	4
Introduction.....	5
Protein lifecycle .....	5
Proteasome .....	5
Loading of peptides .....	7
Listeriolysin O peptidomics .....	7
Purity is everything: how to make a clean protein .....	10
Plasmid generation.....	10
Results .....	11
Protein expression and purification .....	12
Results .....	12
Cellular assays .....	14
Results .....	14
Discussion.....	19
Purification and electroporation .....	19
Generation of non-canonical peptides.....	19
Electroporation as a viable alternative to study the generation of non-canonical peptides in a cellular context.....	19
Materials and methods .....	21
Plasmid generation.....	21
Protein expression and purification .....	21
Cell culture and assays .....	23
References.....	25

## Acknowledgements

This report is an overview of my obtained results during my major internship at the Sijts group in Utrecht. While I am extremely content with the results (both the data obtained and the report itself), I would not have been able to achieve this without some very important people. First off, I would like to thank my daily supervisor Magdalena Wawrzyniuk for her invaluable supervision during my experiments and her push for me to become an independent thinker and scientist. Second, I am very grateful to Alice Sijts for her guidance during the weekly meetings and for giving me the opportunity to do this internship at her group. I would also like to thank both of them, along with Karin Strijbis, for taking the time to read this report and giving me the feedback, allowing me to improve to my maximum potential. Finally, I would like to thank everyone else at the Immunology department for making these some of the most fun and “gezellige” months of my life, but in particular Anne Floor Holtrop for her teatime chats, Youssra Ahidar for all the VMT therapy sessions and Bart van Eshof, Lobna Medfai, Emanuele Nolfi and Daniëlle ter Braake for their mental and physical support, without which I would not have been able to produce this report.

## Introduction

Antigen processing is a process in which an antigen (a molecule, most often a protein) is broken up into pieces (for example peptides) and presented on the cell surface in the form of epitopes. This presentation can then in turn activate a myriad of responses, such as immune activation, antibody production and cell mediated killing. By understanding how our body processes & presents foreign and self-proteins and subsequently prepares its defence upon recognition, we can open up a slew of applications. Currently, antigen processing is mostly used in the development of new vaccines (against pathogens and cancer alike (1)), but there is also a role to be played in the development of immune therapies against cancer (2), autoimmune diseases (3) and perhaps even food allergies (4).

## Protein lifecycle

Most epitopes are derived from the collection of proteins in a cell, also known as the proteome. These proteins perform a variety of roles to keep the cell functioning. Replication of DNA, the uptake of necessary molecules and catalysation of important reactions are just some of the thousands of functions that these proteins perform in the mega factory that is a living cell.

As is the case in a factory, labourers in the cell also grow old and need to be replaced. As such, the proteome is in constant flux, depending on what the cell needs at that time. A protein starts its life cycle when its gene is transcribed from DNA. This produces an RNA strand, which in turn gets transported to a ribosome. Through translation, the RNA is used as a template for the amino acid sequence that make up the protein to be produced. After translation, some modifications are made, after which the protein is ready to perform its function.

The end of this cycle is a process called protein hydrolysis or proteolysis, where proteins are broken down into smaller amino acid sequences called peptides (which can later serve as epitopes on the cell surface). This process is mediated by a modification to the protein called ubiquitination (or ubiquitylation), where a smaller protein named ubiquitin, serving as a tag, is added. This serves as a signal that this particular protein needs to be cleaned up and broken down, at which point it will enter the antigen processing pathway.

## Proteasome

The first step in the antigen processing pathway is the proteasome, a molecular scissor responsible for cutting proteins up into peptides. The proteasome is a barrel-shaped protein complex with a size of 2.5 megadalton (5), comprised of a catalytic core and two regulatory caps on the outside (see figure 1, schematic in figure 2). The caps mediate binding of ubiquitylated proteins, also known as the substrate of the proteasome. After binding, the substrate will be unfolded and deubiquitylated (figure 1A) and translocated into the core, where it will be hydrolysed.



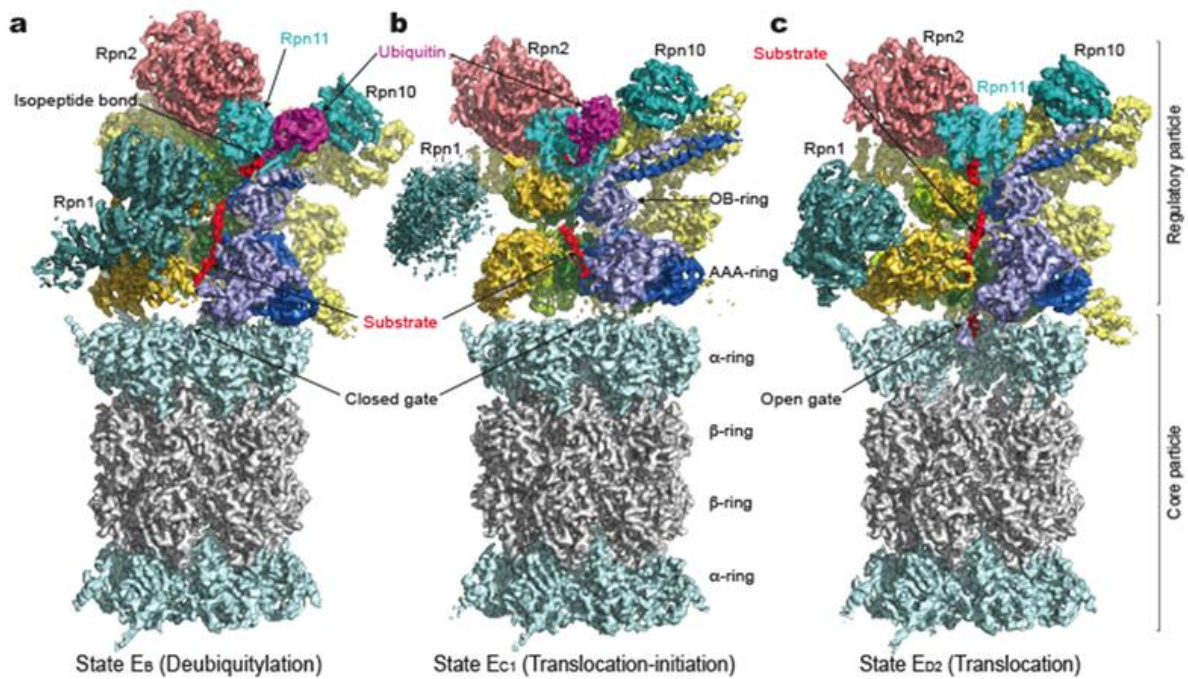


Figure 1: Protein structure in its three known states (A, B and C). Second regulatory unit not pictured. Regulatory cap on top is responsible for binding of the substrate, pushing it into the barrel, where it will be hydrolysed. Source: (5)

The catalytic core of the proteasome is formed by combining two  $\alpha$ - and two  $\beta$ -rings in a barrel shape. The proteasome functions through threonine residues present in the  $\beta$ 1,  $\beta$ 2 and  $\beta$ 5 subunits of its  $\beta$ -rings. As seen in figure 2, the threonine residue performs a nucleophilic attack on the substrate to create an acyl-enzyme intermediate, which will release the rest of the protein (in figure 2 the amino acid with the R3 side group). Afterwards, water (depicted as OH<sup>-</sup> in figure 2) will hydrolyse the acyl-enzyme intermediate, which will release the rest of the protein & return the proteasome to its original state. (6)

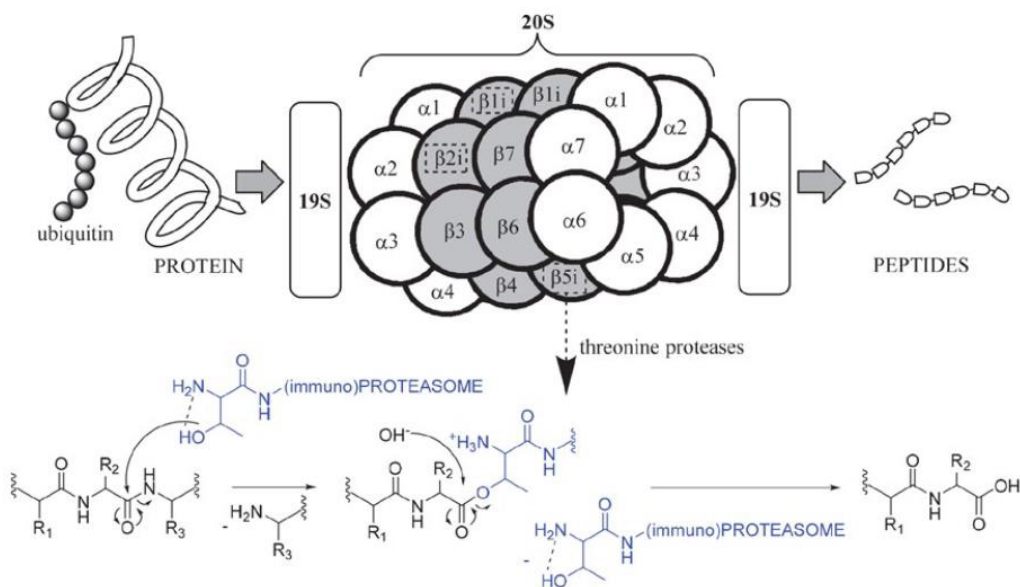


Figure 2: Mechanism of proteolysis in the proteasome. Threonine residues attack the substrate, releasing part of the protein. After hydrolysis by water (OH<sup>-</sup>), the leftover substrate will be released and the proteasome will return to its original state, ready to proteolyze again. Source: (6)

As seen in the schematic drawing of figure 2, the proteasome core consists of a variety of  $\alpha$ - and  $\beta$ -subunits. Under the influence of Interferon gamma ( $\text{IFN-}\gamma$ ), a cytokine produced when the body is in a state of infection, some of these subunits ( $\beta 1$ ,  $\beta 2$  and  $\beta 5$ ) are replaced by their immunoproteasome counterparts ( $\beta 1i$ ,  $\beta 2i$  and  $\beta 5i$ , respectively) (see figure 3). This in turn will create the immunoproteasome, a type of proteasome whose created peptides are better at binding to MHC-I and are thus presented better at the cell surface. (7)

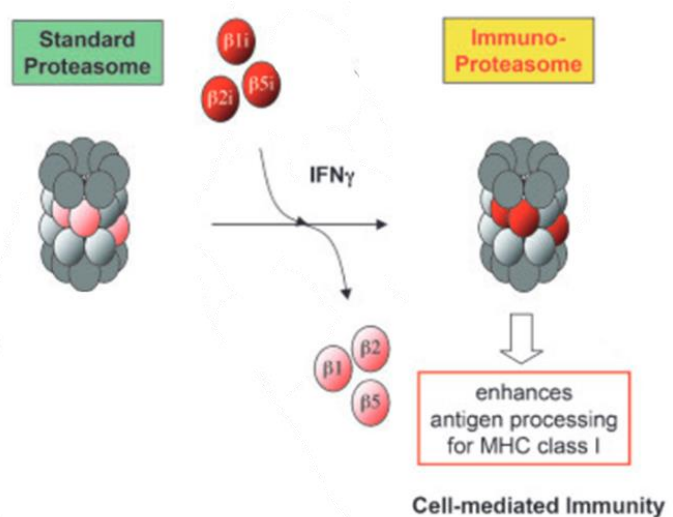


Figure 3: Replacement of  $\beta$ -subunits to create an immunoproteasome, under the influence of  $\text{IFN-}\gamma$ . Adapted from (7).

### Loading of peptides

Now that the cell has generated its peptides, it needs to be presented at the cell surface. This is done by the major histocompatibility complex I (MHC-I) molecules, proteins on the cell surface that function as a silver platter to attach the peptides to, where it can be further recognized by the immune system. As a protein itself, the MHC-I molecules are translated by the ribosome into the endoplasmic reticulum (ER), where they are stabilized by a variety of chaperones. Produced peptides will be transported to the ER by transporter associated with antigen processing (TAP), where it will be loaded on the MHC-I molecule. This loading in turn increases the stability of MHC-I, nullifying the need for the previously mentioned chaperones, that will detach afterwards. The MHC-I molecule is then free to move to the cell surface, where it can be recognized. (8)

The peptide is able to attach to the MHC-I molecule using its so called anchor residues. These residues are of vital importance to the binding to the MHC-I molecule (see figure 4) and vary depending on the type of MHC-I. For example, the H-2Kb subtype of MHC-I seems to either prefer a peptide with a tyrosine (Y) on its fifth position and a small residue at its second position or a peptide with phenylalanine (F) at its fifth position and a hydrophobic residue at its second position. In order to accurately predict potential epitopes, these anchor residues need to be well documented. (9)

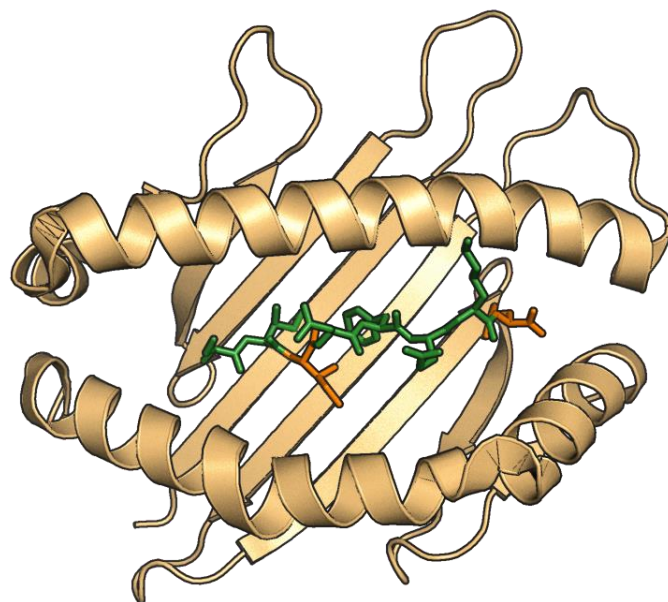


Figure 4: SIINFEKL peptide loaded on the MHC-I molecule (type H-2Kb). The anchor residues are coloured in orange. Figure created by M. Wawrzyniuk

### Listeriolysin O peptidomics

In this research, we use Listeriolysin O protein (LLO) as a model protein. This protein is derived from *Listeria monocytogenes*, a bacterium most known for its danger to pregnant woman (10) and its ability to cause food poisoning (11). The bacteria are capable of infection intracellularly by breaking down the lysosomes in which it is



captured with LLO (12). As such, the protein is present in the cytoplasm during infection by *L. monocytogenes*, enabling it to come into contact with the proteasome and allowing for it to be presented on the cell surface. Through recent techniques like mass spectrometry, it has been possible to more accurately investigate these presented peptides or even peptides digested *in vitro* by purified proteasomes (13). Through this method, it was found that LLO peptides can be produced that should not be possible, based on the linear amino acid sequence of the protein. These so-called non-canonical peptides have no corresponding sequence that can be found in the original, non-processed parent protein or host genome (14). Thus far, there is still debate on how these peptides arise and what factors the process is influenced by.

One suggested theory is that these non-canonical peptides could be products of post-transcriptional RNA editing (15). Additionally, previously presumed non-translating regions of the genome can also produce (faulty) translation products, which are then quickly broken down and also contribute to the cellular peptidome (16).

An alternative non-canonical peptide origin is attributed to a rarely described process known as Proteasome Catalysed Peptide Splicing (PCPS). In this process, the proteasome will paste distant peptides together, instead of just cutting and releasing its substrate as is normally the case. When a substrate is hydrolysed by the proteasome, the acyl-enzyme intermediate will normally be attacked by a water molecule, which will release the substrate. In the case of PCPS, the C-terminal part of the substrate can attack the N-terminal part in place of water, fusing the parts together and creating a novel peptide (17). This newly created spliced peptide (SP) will then function as normal through binding to MHC-I and being presented on the surface. The LLO SP is known to be targeted by CD8+ T cells, suggesting that it can also activate the host's adaptive immunity (18). There are currently thought to be three different versions of PCPS (see figure 5): normal *cis* PCPS, reverse *cis* PCPS and *trans* PCPS. For the purposes of this report, the main focus will be put on normal *cis* PCPS, assumed to be the main way through which the LLO SP arises.

#### Modes of Proteasome-Catalysed Peptide Splicing

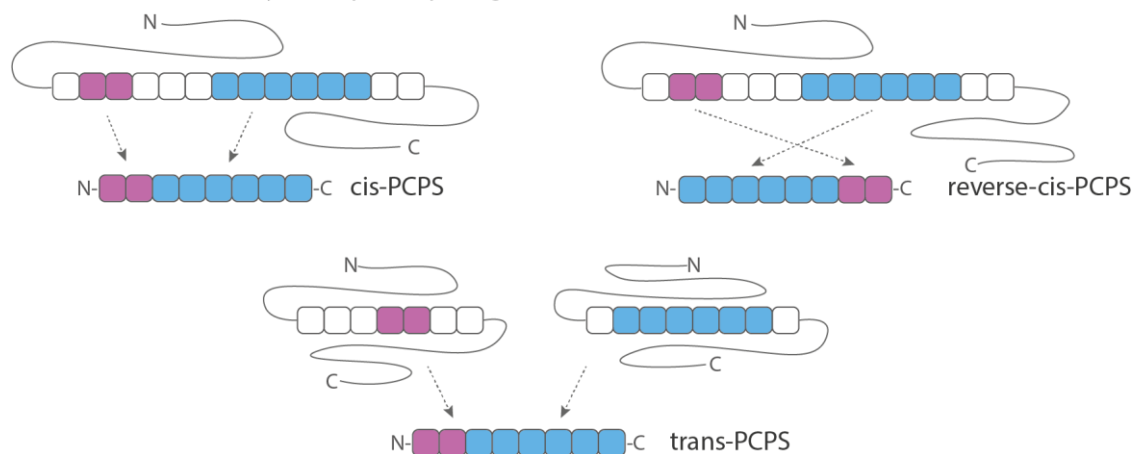


Figure 5: Overview of different types of splicing. During *cis* splicing, the intervening sequence between two distant peptides is removed and the peptides are combined into one. In reverse *cis* splicing, the process is similar, but instead of linear attachment, the peptides are added together in reverse order. In *trans* splicing, two peptides of two separate proteins are added together. Figure created by M. Wawrzyniuk.

In order to investigate the generation of non-canonical peptides *in vivo*, it is important to find a way to introduce the protein into a cell. Currently, the most used method to study (exogenous) proteins is to either electroporate or otherwise introduce a plasmid into cells, from which the protein can be transcribed. However, none of these options eliminate the RNA component to the protein

production. In order to be able to conclude that non-canonical peptides arise through PCPS, it is important to take RNA out of the equation.

Here, a solution is described to further explore the origin of non-canonical peptides, without the use of protein generation involving RNA steps. By producing LLO in *Escherichia coli*, passing it through multiple purification steps to remove any impurities and then electroporating the protein into mammalian cells, the antigen presentation can be studied in cells. Additionally, the LLO SP sequence has been replaced by SIINFEKL to allow easier recognition of the presentation through a variety of assays. This SIINFEKL can then also be split and modified, in an attempt to further elucidate the factors that can influence PCPS. Through these methods, we hope to reduce the uncertainty around the generation of non-canonical peptides and show that Proteasome Catalyzed Peptide Splicing is a viable explanation for this process. Because of the nature of this project, which incorporates both recombinant protein generation and purification with cellular assays, the results are divided over two chapters, in order to be able to equally give weight to both parts.

## Purity is everything: how to make a clean protein

There are two major components to producing an electroporatable protein. The first step is expressing the protein in *E. coli* from a plasmid (see figure 6). After upscaling the cultures, expression of the protein is induced by adding the substance isopropyl  $\beta$ -D-1-thiogalactopyranoside (IPTG), which binds to the LacZ promotor present in the plasmid. The day after, the cultures can be harvested, lysed and their proteins can be purified

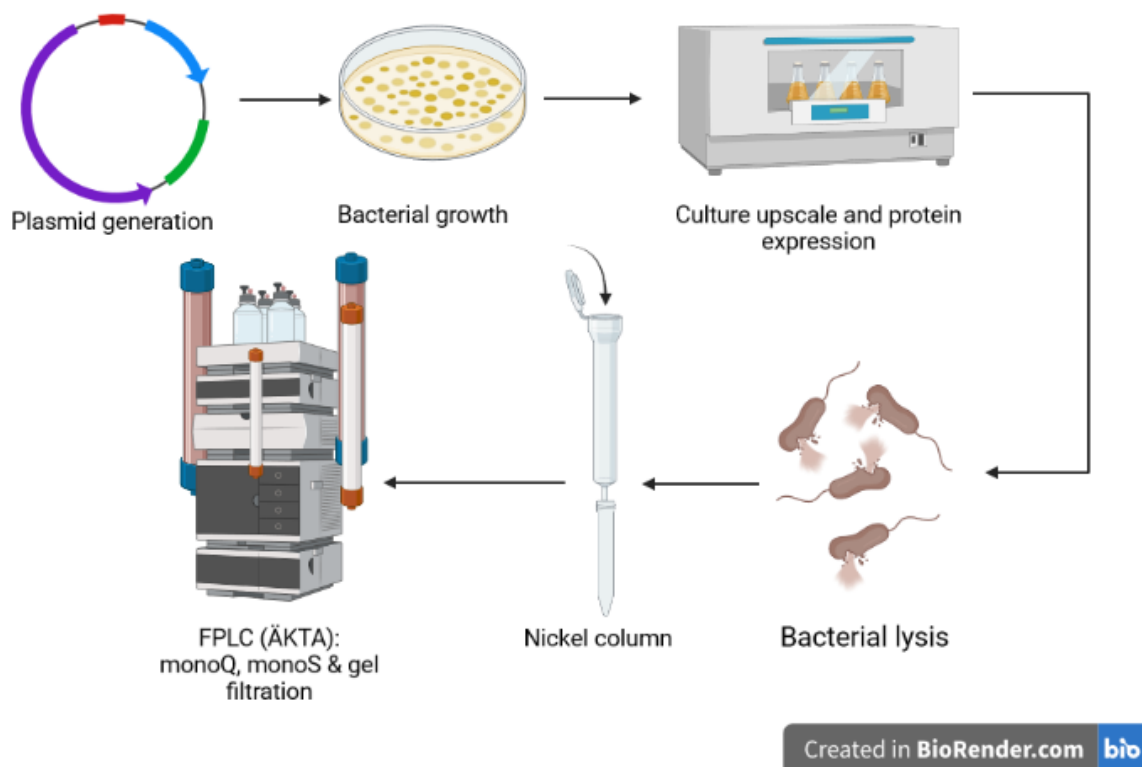


Figure 6: Workflow used for protein production. After successful plasmid generation (verified with sequencing), the plasmid was introduced into the *E. coli* Rosetta strain. The full plate was used to grow a culture, which was scaled up afterwards. Induction of protein production was accomplished by adding IPTG and letting the culture produce protein overnight. Afterwards, bacteria were lysed and the lysate was run on a variety of columns (nickel, monoQ, monoS & gel filtration). Figure created with BioRender.

For the purification, fast protein liquid chromatography (FPLC) was used. The machine, also known as ÄKTA, can separate proteins based on size and charge. However, due to the fact that *E. coli* lysate contains a high amount of LPS, a endotoxin highly toxic to mammalian cells, it is vital to first run the lysate through a nickel column. The His-tag attached to the protein can bind to the nickel present, while other proteins will flush through. Both of these techniques combined produce a highly pure protein sample, which can then be electroporated into mammalian cells.

### Plasmid generation

In order to produce the desired protein, *E. coli* require a template of the required protein in the form of a plasmid. In this research, three different kinds of plasmids were used, being pDONR-221, a small plasmid with kanamycin resistance, and pET160-DEST and pDEST-eGFP-N1-DEST, a plasmid with ampicillin resistance for bacterial expression and a plasmid with kanamycin resistance for mammalian expression, respectively. The starting plasmid used for the creation of the used mutants

was pDONR-221-LLOwt, a pDONR-221 plasmid with a truncated version of wild type LLO inserted. By truncating LLO in this matter, it will lose its toxic properties. Additionally, a pET160-DEST-eGFP and a pET160-DEST-LLO-SIINFEKL (SIINFEKL inserted after the LLO SP) were provided (all sequences provided in the Supplementary Data).

Through a DNA replacement technique (see figure 7), the LLO SP was replaced by the sequence of choice (SIINFEKL shown). To achieve this, primers were designed with a SIINFEKL (or equivalent) tail and a complementary sequence to the flanking parts of the LLO SP.

After two rounds of elongation using these primers, the LLO SP will no longer be present. More elongation steps will result in a higher amount of replaced SP and complementary strands will circularize.

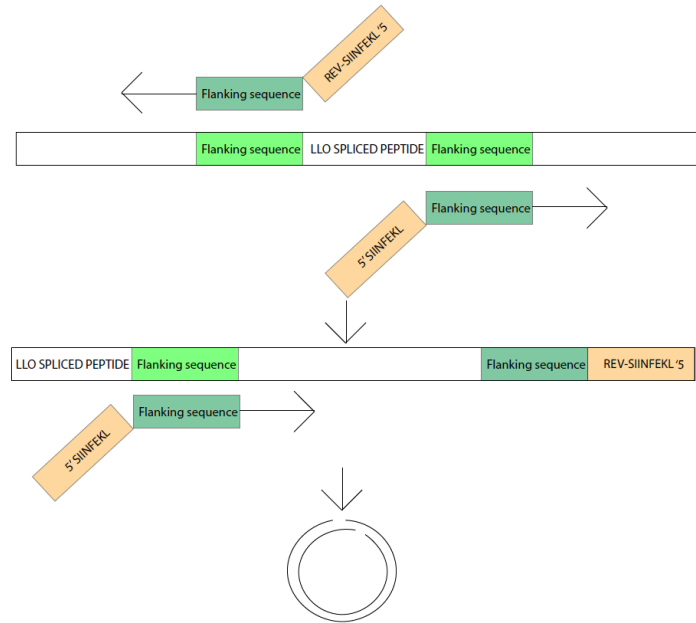


*Figure 7: Schematic representation of the replacement of the LLO spliced peptide with SIINFEKL. A primer was constructed with consensus to the flanking sequence of the LLO spliced peptide. The DNA sequence for SIINFEKL was attached as a tail. After one elongation, there will be a SIINFEKL on one end of the strand and the original spliced peptide on the other. Next round, this last spliced peptide sequence will also be replaced, allowing full linearization of the plasmid.*

## Results

We were successful in the production of SP replaced LLO (rLLO) pDONR-221 plasmids (sequences can be found in the Supplementary Data, for short amino acid sequence see figure 8A). The LR reactions to pET160-DEST were also largely successful. Regrettably, rLLO-SIINFEKL seems to have lost a part of its sequence downstream of the replaced SP. Additionally, because of the low efficiency of the LR reaction into pDEST-eGFP-N1-DEST due to similar antibiotic resistance genes on both the donor and destination plasmid, these plasmids were only created for 3L and 3A. In figure 8B, a result of the LR success check (LR from pDONR-221 into pDEST-eGFP-N1) is shown. On the left, four different colonies of the 3A mutant were loaded. In the following four rows, four different colonies of the 3L mutant were loaded. In the last well, a rLLO-SIINFEKL midiprep was verified. All four 3A plasmids have run further in the gel than the 3L colonies and their size corresponds to the size of the pDONR-221 plasmid (4761 bp). All 3L colonies have run less far in the gel and their size corresponds to the pDEST-eGFP-N1 plasmid (7437 bp).

A

Original peptide: S S V A Y G R Q V Y L K L

Name	AA sequence
rLLO-LIIN	S SVA LIINFE KL
rLLO-SPLIT3A	SIIN SVA FE KL
rLLO-SPLIT3L	SIIN SVL FE KL
rLLO-SPLIT2V	SIIN SV FE KL
rLLO-SPLIT2L	SIIN SL FE KL
rLLO-SPLIT1V	SIIN V FE KL
rLLO-SPLIT1L	SIIN L FE KL

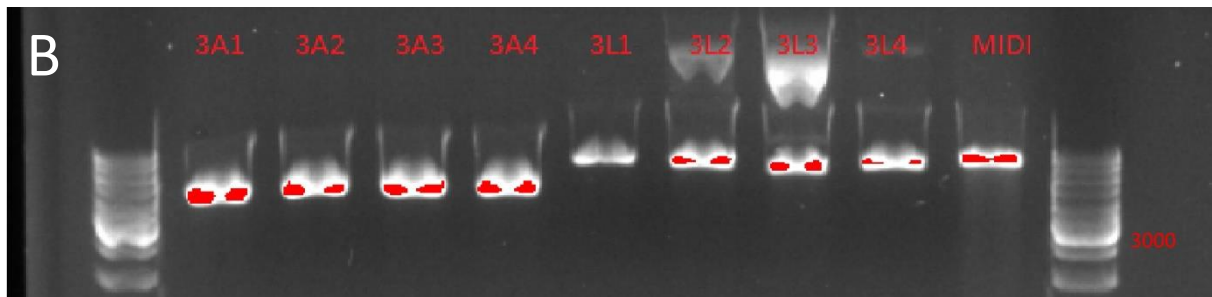


Figure 8: (A) Table showing amino acid sequence of different created mutants. Of these, only rLLO-SPLIT3A and rLLO-SPLIT3L were used in the final experiment. Original amino acid sequence of LLO shown above, with original SP in yellow. (B) Electrophoresis gel after enzymatic reaction with *Nru*I and *Not*I. On the left, four colonies with 3A mutant are shown. Next, four colonies of 3L mutant can be seen. Finally, one well with a midiprep rLLO-SIINFEKL plasmid. The 3A plasmids seem to correspond to the size of the pDONR-221 plasmid (4761 bp). The 3L plasmids seem to correspond to the size of the pDEST-eGFP-N1 plasmid (7437 bp).

### Protein expression and purification

After successful production of bacterial plasmids, we proceeded to the expression and purification steps of the project. For expression, a Rosetta strain of *E. coli* was used, which contains a plasmid encoding different mammalian tRNAs normally not present in bacteria. This eliminates the need for codon optimization in the expression plasmids.

### Results

To eliminate LPS from the protein samples, we loaded the lysate on a Ni-NTA column and a monoQ column on the same day. During the monoQ purification steps, a couple of distinct peaks were visible on the chromatograms (see figure 9A for an example, others can be found in the Supplementary Data). These peaks correspond to proteins that did not attach to the column (not shown in figure), followed by proteins that detach by various salt concentrations, ending with the proteins requiring a large and sudden increase in salt concentration. Along with the proteins, nucleotides and LPS can also attach to the column, usually detaching last due to their high negative charge. These molecules can usually be found in the last peak of the chromatogram. The amount of peaks in the chromatograms suggest that the protein of interest is numerous, but that the injected sample was still unpure. Because of the overlap of the peaks, we can also assume that there is still some un purity

is present after this step. However, due to the negative charge of LPS, we can assume that the sample is now free of LPS and usable for cell assays.

To increase protein purity, we loaded the protein onto a monoS column. After running the fractions of interest on the monoS column, a cleaner chromatogram appears, with a lower amount of peaks (see figure 9B for an example, others can be found in Supplementary Data). The first peak seen on the chromatogram again corresponds with the proteins that did not attach to the column, with the second showing the protein of interest. However, the peak is not fully symmetrical yet, suggesting that there are still impurities in the solution.

In order to have a maximally pure protein, we ran the protein samples on a gel filtration column. The chromatogram for this process (Figure 9C) is cleaner compared to monoQ and monoS and shows a more symmetrical peak. In order to get the most purity, only fractions of the symmetrical part of the peak are taken.

To check the purity of the fractions, we performed a gel electrophoresis and a Coomassie stain (Figure 9D, E, F). The Coomassie shows less impurities after every purification step, however some samples still show small amount of impurities. Combining this with the fact that we ran the samples on all possible columns, we conclude that the samples are now as pure as possible and are able to be used for the cellular assays.

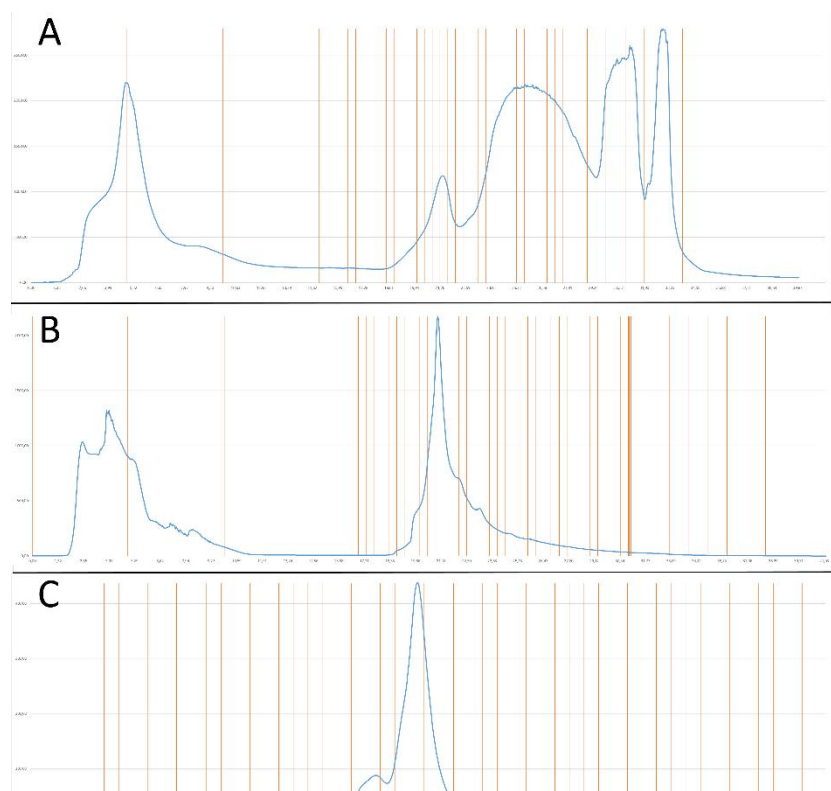


Figure 9: Results of purification steps with Coomassie stainings to show increase in purity. **(A)** MonoQ chromatogram of rLLO-SPLIT3A. From left to right, different peaks represent the flowthrough of the column [Fractions X1-X2], proteins with a more positive charge than rLLO-SPLIT3A [Fraction B2], peak representing rLLO-SPLIT3A [Fractions B11 and C5] and two peaks representing leftover protein with a higher negative charge and negatively charged molecules [Fraction C10]. **(B)** MonoS chromatogram of rLLO-SPLIT3L, showing the difference in purity compared to monoQ. In this chromatogram, only a peak for flowthrough and the protein of interest are visible. Peak for protein of interest is still asymmetrical, suggesting that there still is some impurity **(C)** Gel filtration chromatogram for rLLO-SPLIT3L showing a symmetrical peak with only a small asymmetrical bump. By only taking fractions of the big peak, maximum purity is reached. **(D)** Coomassie stain for fractions from first chromatogram shown (last peak not shown), with LLO mutants showing up between 20-25 kDa. Fractions B2 and C10 do not show protein of interest, while B11 and C5 do, along with more impurities. **(E)** Coomassie stain of fractions obtained in (B) showing higher purity in fractions B1 to B4. **(F)** Coomassie stain of proteins after gel filtration. rLLO-SIIN, rLLO-3L and rLLO-3A show high purity, but LLO WT has impurities and does not seem to have protein of interest.



## Cellular assays

To explore PCPS in a cellular context, two different cell lines were used. The proteins of interest need to be delivered inside the antigen presenting cells (APCs) and be given time to be digested, after which our peptide of interest should become presented on the cell surface. Since delivery of proteins is done through electroporation, preliminary experiments were done on the murine melanoma cell line B16, a cell line that can be efficiently electroporated and is relatively resistant against the damage of the electric shocks, as evidenced by experiments shown below. In later experiments, the murine macrophage cell line Ana1 was used, after it was found to have superior expression of H-2Kb on its surface, evidenced by FACS staining experiments.

To quantify the amount of PCPS derived SIINFEKL expression on the cell surface, two different techniques are available. A FACS staining using antibody 25-D1.16, reacting with SIINFEKL bound to H-2Kb, or assays using the reporter cell line B3Z can be performed. The B3Z cell line, created by fusing the NFAT-lacZ reporter construct expressing Z.8 cell line with the B3 T cell line expressing a receptor for SIINFEKL (19), is a very sensitive reporter of SIINFEKL bound to H-2Kb. Upon recognition of the peptide, B3Z will produce the LacZ enzyme, which can transform the dye CPRG into CpR, after lysis of the cells. This transformation causes a colour shift, which can be measured by exciting the mixture at 595 nm (Figure 10).

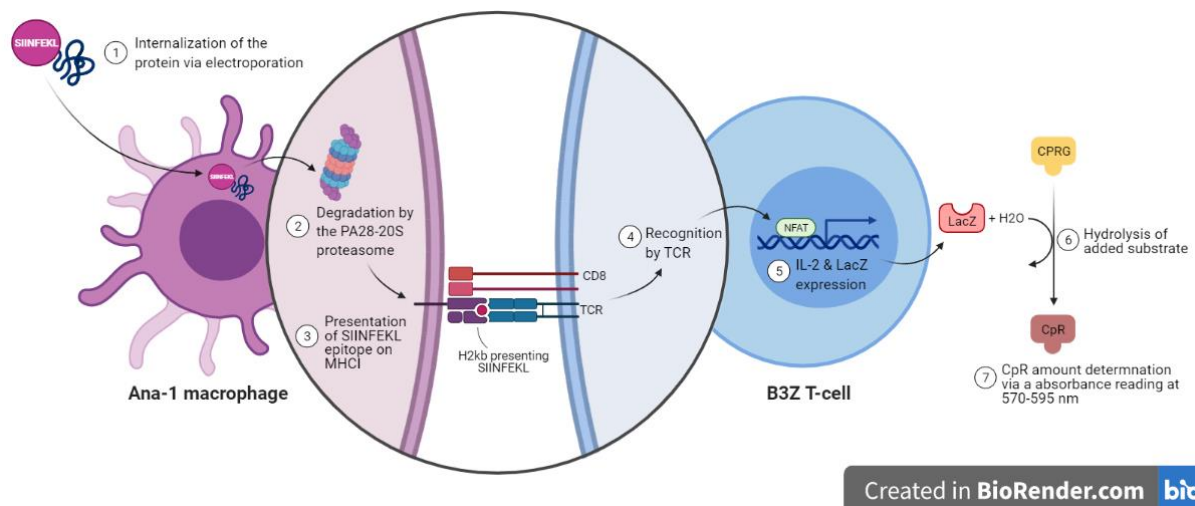


Figure 10: In this figure, the working mechanism of B3Z is shown. Upon recognition of the SIINFEKL antigen, the B3Z will produce an enzyme that will interact with the dye CPRG. If incubated for 4 to 5 hours at 37C, a change of absorbance can be shown in a plate reader. Figure made by A.F. Holthrop using BioRender.

## Results

In order to judge if antibody staining is a viable method to quantify SIINFEKL presented on the surface, we stained B16 WT and B16OVA using the 1:50 PE-conjugated 25-D1.16 antibody (Figure 11A). In the case of B16 OVA, there is a very minimal small shift visible on the PE spectrum. Solely based on these results, we concluded that FACS is not an effective method for quantifying SIINFEKL expressed on the cell surface.

Additionally, in order to optimize peptide loading steps in later experiments, we performed a peptide loading FACS staining using the same antibody concentrations (Figure 11B). A slightly bigger shift is visible compared to the B16OVA experiment, peaking around a peptide concentration of 1  $\mu$ M and 1 nM. From this, we concluded that the antibody staining is effective, but only when high concentrations of SIINFEKL are presented on the cell surface. Additionally, a peptide concentration of around 1  $\mu$ M to 1 nM seemed to be optimal and was henceforth used as the positive control for further experiments.

To optimize protein concentrations in later electroporation experiments, we performed a pilot experiment using monoQ-purified eGFP. In this experiment, we electroporated cells with different concentrations of eGFP (20, 10, 4, 2 and 0  $\mu$ M), performed several washing steps to remove outside eGFP and ran the samples on FACS to see shifts in the eGFP channel (figure 12A). While all the samples shifted upwards, 20 and 10  $\mu$ M of eGFP seemed to give the best results. Since the shift is similar in both samples, this suggested peak saturation, so 10  $\mu$ M concentration was used for further experiments from this point on.

Additionally, we took pictures using the fluorescent microscope in a later experiment, using the previously established 10  $\mu$ M optimal concentration to electroporate both B16 (Figure 12B) and Ana1 (Figure 12C). Based on these pictures, we concluded that most of the eGFP located intracellularly, with small clumps of eGFP still present extracellularly.

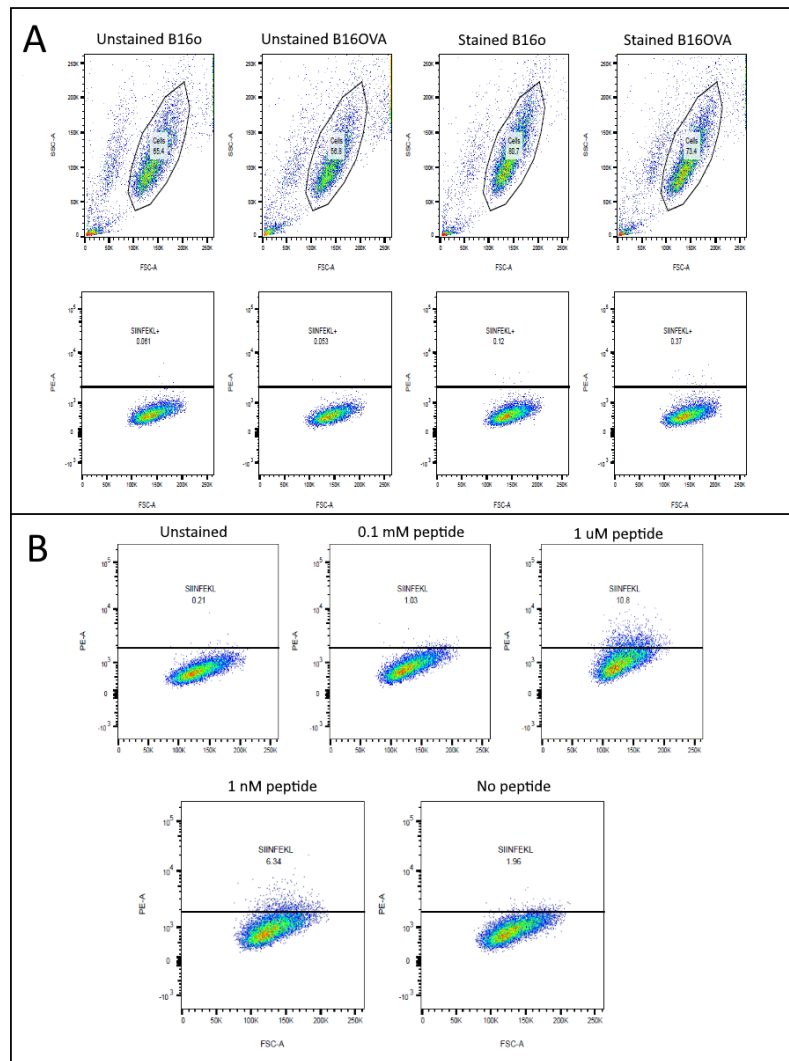


Figure 11: FACS results using the SIINFEKL in H-2KB antibody. (A) Staining done on B16 WT (B16o) and B16OVA. A small shift is visible on the PE spectrum when B16OVA is stained compared to the controls. (B) Staining done on cells loaded with SIINFEKL peptide. A large shift is visible when cells were loaded 1  $\mu$ M and 1 nM peptide in the medium.

To obtain optimal cell concentrations of APCs (B16 or Ana1), B3Zs and medium conditions, we performed a variety of assay optimization experiments. As a basis for the experiment, we referred to the protocol used by Karttunen et al. (19). In the first of these experiments, we varied the amount of B3Z per well added (Figure 13A), following the established protocol for the rest of the variables ( $1 \times 10^4$  B16s per well, 200  $\mu$ L volume, IMDM with 10% heat inactivated foetal calf serum, 1% penicillin/streptomycin and 0,1%  $\beta$ ME).  $1 \times 10^4$  B3Z cells per well gave a 1,2 fold change in absorbance compared to the negative control.  $2 \times 10^4$  B3Z cells per well fared slightly better, giving a 1,4 fold change in absorbance compared to the negative control.  $3 \times 10^4$  cells per well and  $7,5 \times 10^4$  cells per well gave the biggest fold change, being 1,8 and 1,6 respectively. Based on these results, we established that the optimal B3Z density seemed to be around  $3 \times 10^4$  cells per well.

To explore optimal APC densities, we serially diluted the B16/B16OVAs used in the assay, starting at the  $1 \times 10^4$  cells per well established in Karttunen et al. Additionally, in this experiment we also tried to optimize B3Z concentrations further, seeding  $3 \times 10^4$  B3Z cells per well and  $5 \times 10^4$  B3Z cells per well.

While  $1 \times 10^4$  B16 cells per well gave a 2-fold change,  $1 \times 10^3$  cells per well produced a 2,5 fold change compared to the negative control. As such, we concluded that both  $1 \times 10^4$  and  $1 \times 10^3$  cells per well were usable densities. Additionally, fold change was similar for both B3Z densities, so we concluded that both  $3 \times 10^4$  B3Z cells per well and  $5 \times 10^4$  B3Z cells per well were usable (Figure 13B).

In the final optimization experiment, we wanted to re-test the APC optimization conclusions along with exploring the effect of different concentrations of IFN- $\gamma$  (25, 50, 75 and 100 ng/mL) on the assay. In this experiment,  $1 \times 10^3$  cells per well seemed to give a lower fold change overall compared to  $1 \times 10^4$  cells per well. On top of this, adding IFN- $\gamma$  did not seem to show drastic effects on the presentation of SIINFEKL on the cell surface, showing similar fold change for all concentrations. Based on these results, we established that  $1 \times 10^4$  B16 cells per well is an optimal density and that adding different concentrations of IFN- $\gamma$  did not have a significant effect.

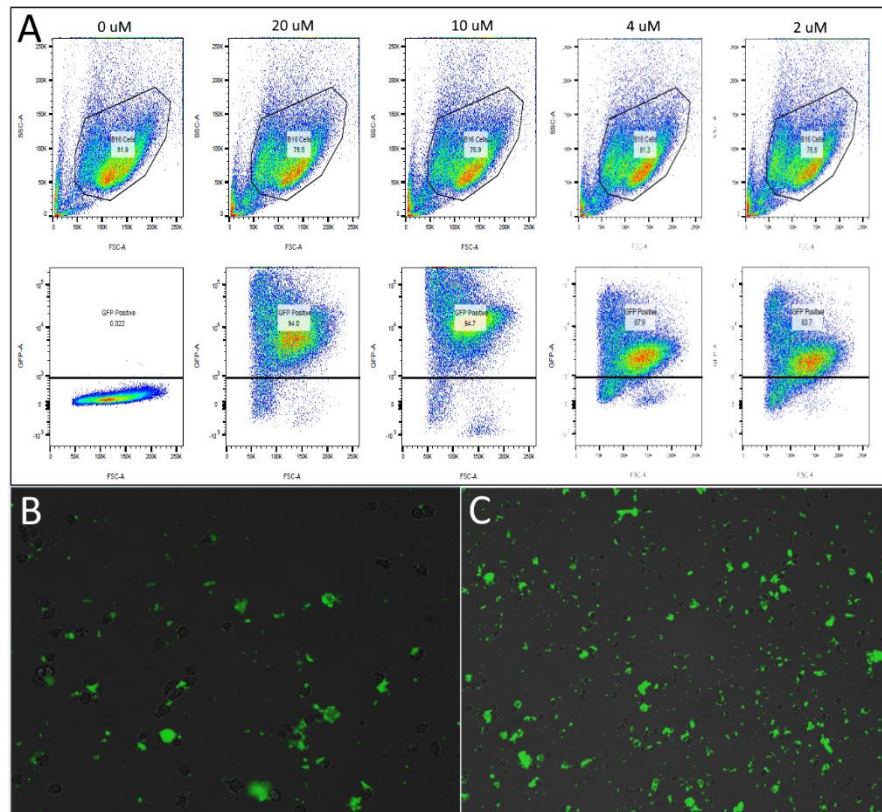


Figure 12: Results of eGFP electroporation experiments. (A) FACS results of electroporation with concentrations of 20, 10, 4, 2 and 0  $\mu$ M. 20 and 10  $\mu$ M eGFP gave an increased shift compared to 4 and 2  $\mu$ M. The shift in the 20 and 10  $\mu$ M was comparable, suggesting peak saturation of the protein concentration. (B) Fluorescent picture of B16 cells electroporated with 10  $\mu$ M eGFP. (C) Fluorescent picture of Ana1 cells electroporated with 10  $\mu$ M eGFP.

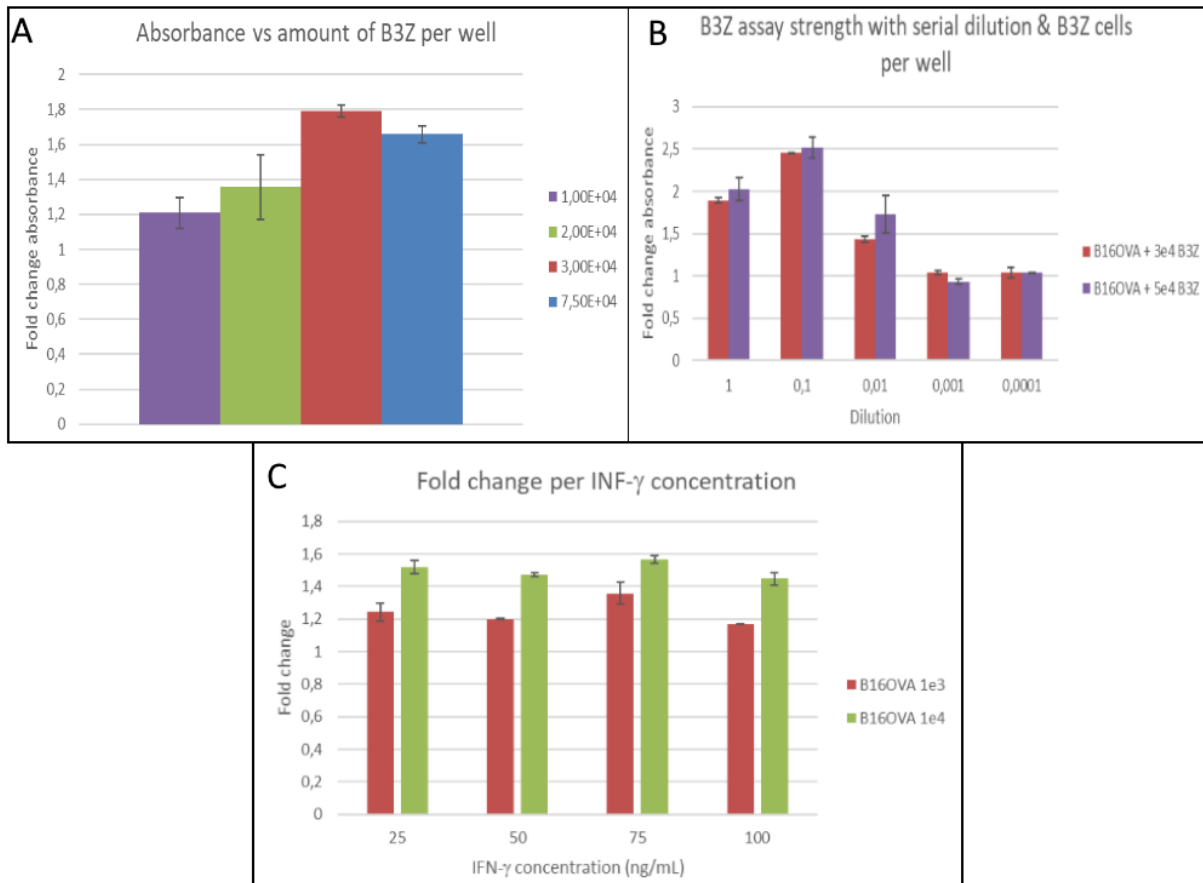


Figure 13: Optimization results of B3Z assays. All data is normalised to the average of the negative control (B16, not shown) and averaged per condition. Error bar shows the standard deviation. In all these experiments, B16OVA was used. (A) Absorbance shown for different cell densities of B3Z ( $1 \times 10^4$ ,  $2 \times 10^4$ ,  $3 \times 10^4$  and  $7,5 \times 10^4$  B3Z cells per well, rounded off.) Densities between  $3 \times 10^4$  and  $7,5 \times 10^4$  B3Z cells per well seemed optimal. (B) Optimization to test assay strength with decreasing amount of APCs, using a 1:10 serial dilution, starting at  $1 \times 10^4$  cells per well. Optimal amount of APC density seemed to be around  $1 \times 10^4$  and  $1 \times 10^3$  cells per well. Additionally, previous result of optimal B3Z amounts was corroborated, showing similar results for  $3 \times 10^4$  and  $5 \times 10^4$  B3Z cells per well. (C) Optimisation to show effect of 25, 50, 75 or 100 ng/mL IFN- $\gamma$  on B3Z assay, with minimal differences between each concentration.

By combining all the previously established results and optimisations, we have achieved an optimal assay for showing potential PCPS-derived SIINFEKL expressed on the cell surface. For the final assay, we electroporated Ana1 with four different proteins, being eGFP, rLLO-SPLIT3A, rLLO-SPLIT3L and LLO-SIINFEKL. In this context, eGFP serves as a negative control with no SIINFEKL expression. rLLO-SPLIT3A and -3L are the proteins which do not have SIINFEKL in its contiguous form and which can only show SIINFEKL on the cells surface if PCPS happens. LLO-SIINFEKL serves as a positive control for the electroporation, since it should always give a signal if electroporation worked. Finally, cells electroporated with eGFP were seeded in a final column of wells and loaded with 1  $\mu$ M peptide, to serve as a positive control for the B3Z functionality. In the results of this assay (Figure 14), an increase can be seen in all different conditions. The peptide loaded wells (strongest positive control to ensure B3Z activity) show the highest fold change, being around 4,25. The APCs electroporated with LLO-SIINFEKL also give a high fold change, being around 2,15. Both 3A and 3L seem to show a fold change, being around 1,25 and 1,5 respectively. Based on these results, we can conclude that SIINFEKL seems to be present in all conditions except the negative control, albeit more numerous in the positive controls.

### Fold change absorbance of electroporated proteins compared to eGFP negative control

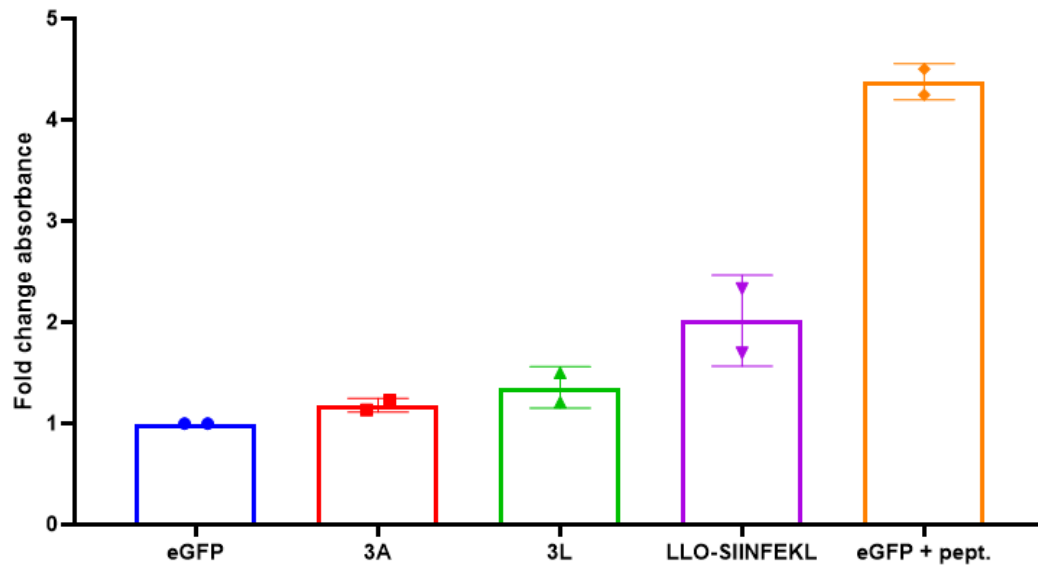


Figure 14: Results of the B3Z electro-assay using the rLLO-SPLIT mutants. rLLO-SPLIT3A and 3L both seem to show a small increase compared to the negative control. Peptide loading was used as a control for the functionality of the assay, LLO SIIN was used as a control for the electroporation. All samples averaged and normalised to negative control. Error bars show standard deviation.

## Discussion

### Purification and electroporation

Currently, electroporation of proteins is not widely used. It mostly enters the spotlight when DNA/mRNA electroporation is not sufficient, such as in the case when the protein of interest needs to be expressed before any transcription/translation could have taken place. This can be seen in the case of embryonic CRISPR-Cas9 experiments, where Cas9 introduced in DNA or mRNA form will only be expressed after some rounds of DNA replication have already taken place, causing genetic mosaicism (20). Additionally, expression of proteins from plasmids can possibly yield too low of a signal for readout, especially in the case with low cell amounts (21).

Protein production and purification is not a “one size fits all” process. Most proteins used for electroporation are either commercially ordered (20) or only purified by using Ni-NTA columns and extensive washing to remove leftover LPS (21). However, in the case where the protein is not commercially available or a higher purity is needed, a low-affinity column such as Ni-NTA is not sufficient. As such, it is essential to incorporate FPLC into the purification methods, to obtain a higher protein purity (22). In our experiments, we have shown that by using FPLC, we can obtain a high purity protein which can be electroporated into cells.

### Generation of non-canonical peptides

Previously, it was already established that non-canonical peptides and the LLO SP could be generated *in vitro* using LLO-derived polypeptide substrates and purified proteasomes (14). Relevance in an immunological context was also shown by the identification of reactivity to spliced epitopes by CD8+ T cells, after infection with *L. monocytogenes* (23). By combining the electroporation techniques with the B3Z assay, we have established that this process is also able to take place intracellularly. Due to the absence of DNA/RNA in the protein samples, we are also able to conclude that the non-canonical peptides were not generated as a consequence of RNA editing (15) or derived from noncoding regions in the genome (16). Taken together, this implicates that Proteasome Catalysed Peptide Splicing can be a source of non-canonical peptide splicing in the cell, independent of the transcription-translation process.

### Electroporation as a viable alternative to study the generation of non-canonical peptides in a cellular context

In this report, we have shown that electroporation of proteins is an effective and viable alternative to DNA electroporation and viral vectors to get proteins inside a cell. We have shown that cells electroporated with protein are still able to process this protein using its proteasome and express peptides derived from the electroporated protein on the cell surface. Subsequent antigen recognition by specialised cells is also present, as was also seen in the research done by Chen et al. (24)

Additionally, we have indication that splicing can happen *in vitro* with a peptide that was not originally present in the protein. Papers studying factors involved in splicing focus on the internal amino acid sequences of the spliced peptide and try to extrapolate from that if there are optimal amino acids at optimal positions (25). However, by removing and replacing the internal sequence of the original LLO SP, we can focus more if the flanking sequences around the peptide are important. As we have seen that splicing is still present without the same internal sequence, it would seem that the internal amino acid sequence is not solely responsible for the splicing process. Instead, the flanking sequences present in LLO seem to be (in part) responsible for allowing the proteasome to create non-canonical peptides.



Through the generation of rLLO-SPLIT mutants, we have created a model protein that can be used in future research into PCPS. By making minor changes to the protein, it is possible to study the factors involved in PCPS in more detail. New mutants could contain mutations to the internal or flanking regions of the SP or a relocation of SPLIT-SIINFEKL to different positions in the protein. Additionally, since the rLLO-SPLIT3L mutant showed a higher fold change compared to the rLLO-SPLIT3A mutant, mutations in the linker sequence can also prove to be an avenue for better understanding of the mechanism behind PCPS. Taking inspiration from studies identifying common splicing factors (26), an increase or decrease in the amount of linker amino acids could also be a modification worth looking at. Finally, by swapping around the order of the SP, opportunities to study *reverse cis* or even *trans* splicing could open up.

Additionally, we hope that the results on the electroporation of proteins will entail a change in the current thinking around protein delivery to cells. A fully produced and purified protein can prove itself to be extremely useful in studying the effect of processes like glycosylation, ubiquitination and other post-translational modifications in cellular environments.

## Materials and methods

### Plasmid generation

To achieve replacement, 2,5  $\mu\text{L}$  of 0,01 nM forward and reverse primers (Invitrogen/Thermofisher) (for sequence see Supplementary Data) was added to 50 to 100 ng of plasmid and a mastermix [10  $\mu\text{L}$  5x polymerase buffer (New England Biolabs), 2,5  $\mu\text{L}$  of 4 mM dNTPs, 2,5  $\mu\text{L}$  of DMSO and 0,7 units of Q5 polymerase (New England Biolabs)] and topped up to 50  $\mu\text{L}$  with MilliQ. Subsequently, the sample was inserted into a T100 Thermal Cycler (Biorad) and put through the following PCR program (AT1 = annealing temperature of the flanking sequence, AT2 = annealing temperature of the whole primer): 95  $^{\circ}\text{C}$  for 3 minutes, a cycle of 30 seconds of 95  $^{\circ}\text{C}$  – AT1 for 30 seconds – 72  $^{\circ}\text{C}$  for 5 minutes, repeated 12 times. Afterwards, the cycle was repeated with AT2, for 22 times. Finally, the sample was heated to 72  $^{\circ}\text{C}$  for 5 more minutes. Through digestion with 10 units of DpnI (New England, Biolabs) for 75 minutes at 37  $^{\circ}\text{C}$ , the methylated template plasmid was removed. 5  $\mu\text{L}$  of DNA was used to transform Top10 bacteria, which were plated out on an agar plate containing kanamycin (Biotrading). Single colonies were picked out, grown in Luria Broth (LB) medium (Biotrading) containing 50  $\mu\text{L}/\text{mL}$  kanamycin and the plasmid was purified from these cultures using miniprep (Zymo Research, USA). To verify success of the PCR, the plasmids were sequenced by MacroGen Sequencing.

In order to study splicing, mutants where SIINFEKL was not originally present were desired. Based on previous research (26), it was decided to split SIIN/FEKL with either 1, 2 or 3 intervening amino acids, chosen based on the intervening amino acids in the LLO SP (from hereon called LLO-SPLIT or SPLIT for short). Additionally, for each mutant another variant was made where the last amino acid was replaced by a leucine (L). This yielded the final 6 mutants SPLIT1V, SPLIT1L, SPLIT2V, SPLIT2L, SPLIT3A and SPLIT3L, with the final letter representing the last intervening amino acid (full sequences can be found in the Supplementary Data).

To transfer the coding sequence from pDONR-221 to the destination plasmids (pET160-DEST, pDEST-eGFP-N1-DEST), an LR reaction was used, via the attL sites in pDONR-221 and attR sites in the destination plasmids. 100 ng of pDONR-221 plasmid was added to 100 ng of the destination plasmid, along with 2  $\mu\text{L}$  of LR clonase enzyme mix (Invitrogen/Thermofisher) and topped up to 10  $\mu\text{L}$  with TE buffer (Invitrogen/Thermofisher, Germany). The sample were vortexed 2 times briefly and left at 22  $^{\circ}\text{C}$  overnight. Afterwards, 1  $\mu\text{L}$  of Proteinase K (Invitrogen/Thermofisher) was added and put on 37  $^{\circ}\text{C}$  for 10 minutes. Top10 bacteria were transformed with 3,5  $\mu\text{L}$  of the mix and plated on either ampicillin plates or kanamycin plates (Biotrading), depending on the resistance in the destination plasmid. Single colonies were picked, grown in liquid LB medium with corresponding antibiotic [50  $\mu\text{L}/\text{mL}$  for kanamycin, 100  $\mu\text{L}/\text{mL}$  for ampicillin (Sigma-Aldrich, China)] and miniprep was used to harvest their plasmids.

LR success was checked by adding 200 ng of plasmid to 5 units of an enzyme cutting each plasmid once [NruI (New England Biolabs) for pDONR-221 and pET160-DEST, NotI (New England Biolabs) for pDEST-eGFP-N1-DEST], 2  $\mu\text{L}$  3.1 buffer (New England Biolabs) and topped up to 20  $\mu\text{L}$  with MilliQ. The coding sequence was also checked using MacroGen sequencing. Successful plasmids were upscaled using the midiprep (Biorad, USA) protocol. On top of the normal forward sequencing, the midiprepped plasmids were also sequenced in reverse to ensure the validity of the inserted sequence.

### Protein expression and purification

To begin the expression, 50 to 100 ng of plasmid was added to the bacteria and incubated for 10 to 20 minutes on ice, mixed from time to time by tapping the Eppendorf. Subsequently, the bacteria

were heatshocked for 90 sec at 42 °C and placed on ice for 1 minute after. 400 µL of 37 °C SOC medium (Invitrogen, Carlsbad USA) was added and the bacteria were incubated for 50 min at 37 °C, shaking. The bacteria were then plated on an agar plate containing ampicillin and put at 37 °C overnight.

The following day, the entire plate was used to inoculate 100 mL of LB or Terrific Broth (TB) (Sigma-Aldrich, St. Louis USA) containing 100 µL/mL ampicillin and 37 µL/mL chloramphenicol (Sigma-Aldrich, Belgium) and put at 37 °C for 1.5 hours. Afterwards, the preculture was scaled up to 800 mL using the same LB medium and incubated until the OD600 reached 1 – 1.5. This culture was then divided in four parts of 200 mL and 600 mL of fresh medium was added. When the OD600 reached 0.6 – 0.8, the cultures were cold shocked on ice for 10 minutes. Protein expression was induced by adding 200 µL 1M IPTG (Invitrogen, Italy) and incubated at 28 °C overnight. To harvest the bacteria, an equal amount was distributed to four centrifuge buckets and spun down at 4 °C, 5311 G for 20 minutes. The supernatant was removed, the cell pellet was harvested using cold PBS and stored at -80 °C.

The pellet was lysed by adding 1 to 2 mL of lysis buffer [50 mL PBS (Corning, USA), 5 mM of magnesium chloride hexahydrate (Sigma-Aldrich), 100 µL of 2 mg/mL DNase I (bovine pancreas origin, Sigma-Aldrich), 50 mg lysozyme (Sigma-Aldrich), 50 µL Tween-20 (Merck, Darmstadt Germany, produced in France) and 5 mM of βME (Millipore Corp., Bedford MA USA)] and shaking for 10 minutes. The pellet was then refrozen at -80 °C for 20-30 min and thawed in tap water, repeated up to 5 times. If the pellet was not lysed sufficiently (judged by fluidity of the pellet), 0,1% of total lysate volume Tween-20 was added, along with 1 mg/mL lysozyme and incubated at 22 °C for 45 min, shaking. The lysate was then transferred to a Beckman centrifuge tube and spun in a fixed angle centrifuge at 48000 RCF, 4 °C for 50 minutes. A 20 µL sample of the supernatant for a Western Blot was taken afterwards.

A Ni-NTA column was prepared by washing with at least 5 column volumes (CV, 8 mL) of MilliQ and equilibrated with at least 5 column volumes of Ni-NTA binding buffer [1 proteinase inhibitor tablet (Roche, Mannheim Germany) and 2,5 mM β-mercaptoethanol added to 250 mL of PBS]. The lysate supernatant was passed through a 0,22 µm filter and loaded onto the column. After passing the flowthrough, another 20 µL sample was taken and the flowthrough was loaded again. After another passage, an additional 20 µL sample was taken. Subsequently, the column was washed with 5 to 10 times the column volume with Ni-NTA washing buffer [0,1% Tween-20 added to 25 mL of Ni-NTA binding buffer] and eluted by adding 6 mL of elution buffer [0,5 M of imidazole (Merck, Darmstadt Germany) added to Ni-NTA binding buffer]. Afterwards, one final 20 µL sample was taken.

FPLC was done in three distinct steps, starting with a MonoQ IEX column. 2x stock buffers for buffer A [50 mM NaCl, 50 mM Na-P, pH = 7,2 in MilliQ] and buffer B [4 – 6 M KCl in MilliQ] were prepared and were used to create the 1x buffers by adding MilliQ and 2x buffer in equal parts, along with 5mM β-mercaptoethanol for both buffers and ½ proteinase inhibitor tablet for buffer A. The protein was then purified using the MonoQ protocol [CV = 0,982; 10% buffer B gradient over 12 CV with 0,4 mL fractions; 80% buffer B gradient over 5 CV with 1 mL fractions; 100% buffer B gradient over 0 CV, 1 mL fractions]. Afterwards, 2x buffer A for MonoS was prepared by adding 40 mM MESE, 40 mM NaCl to 1 L MilliQ. 1x buffer was prepared in the same way as in the previous step. Using a buffer exchange tube, the protein was transferred from MonoQ buffer B to MonoS buffer A. The MonoQ column was swapped for a MonoS column and the protein was purified using the MonoS protocol [CV = 0,982; 80% buffer B gradient over 12 CV with 0,4 mL fractions; 100% buffer B gradient over 0 CV, 1 mL fractions]. Finally, a gel filtration was performed using 0,22 µm filter sterilised protein storage buffer [150 mM NaCl (Merck Darmstadt, produced in Denmark), 20 mL of glycerol (Merck

Schuchardt OHG, Hohenbrunn Germany), 5 mM of  $\beta$ -mercaptoethanol and 1 proteinase inhibitor tablet added to 180 mL of PBS]. Purity of the fractions was checked by running the fractions and the samples taken earlier on a gel and performing a Coomassie stain.

### Cell culture and assays

All B3Z cells and B16-derived cells were cultured in IMDM full medium [10% heat inactivated foetal calf serum (FCS) (Bodinco B.V., The Netherlands), 1% penicillin/streptomycin (Life Technologies Ltd., Paisley, Scotland, UK / Gibco) and 0,1%  $\beta$ ME added to IMDM (Life Technologies Ltd., Paisley, Scotland, UK / Gibco)]. Additionally, all Ana1 cells were cultured in RPMI full medium [10% heat inactivated foetal calf serum (FCS) (Bodinco B.V., The Netherlands), 1% penicillin/streptomycin (Life Technologies Ltd., Paisley, Scotland, UK / Gibco) and 0,1%  $\beta$ -mercapto-ethanol ( $\beta$ ME) (Millipore) added to RPMI-1640 (Life Technologies Ltd., Paisley, Scotland, UK / Gibco)]. When cells of different media were co-cultured, RPMI full medium was used. Cells were grown in a humidified incubator (Binder, Tuttlingen Germany) with an atmosphere of 5% CO<sub>2</sub>, at 37 °C.

For early optimizations, B16 derived cell line B16-OVA, a B16 cell line expressing the SIINFEKL peptide, was used as positive control. This cell line was created by stably transducing B16 with the ovalbumin gene using a lentivirus vector. Later on, this was replaced by loading B16 cells with SIINFEKL peptide (Genscript, stock concentration 10 mg/mL), by adding the desired concentration to cell culture medium.

To show SIINFEKL presented on the cell surface, 2e5 to 1e6 cells were stained using a 1:50 dilution of PE-conjugated OVA257-264 (SIINFEKL) peptide bound to H-2Kb Monoclonal Antibody (Invitrogen/ThermoFisher, USA) following normal external staining protocols. Subsequently, fluorescence was measured on BD FACSCantoII (BD Biosciences, San Jose USA) and analysed using FloJo.

To achieve protein delivery through electroporation, cells were harvested following their advised protocol and concentrated to 4 x 10<sup>6</sup> cells in 200  $\mu$ L (for B16) or 1 x 10<sup>7</sup> cells in 200  $\mu$ L (for Ana1), washed in serum free RPMI [1% penicillin/streptomycin and 0,1%  $\beta$ ME added to RPMI-1640 (Life Technologies Ltd., Paisley, Scotland, UK / Gibco)] and resuspended in serum free RPMI. Cells were transferred to electroporation cuvettes and 10  $\mu$ M of protein was added. After a rest period of 3 to 5 minutes, cells were electroporated using a Bio-Rad Gene Pulser II Electroporator, at 250V, 975  $\mu$ F and infinite resistance. After electroporation, cells were given 3 mL of 2x medium (37 °C) [10% heat inactivated FCS, 2% penicillin/streptomycin and 0,1%  $\beta$ ME added to the respective media] to compensate for unsterile protein and left to recover for 3 minutes. Afterwards, cells were spun down at 300 RCF for 4 minutes at 21 °C, resuspended and used for further experiments.

For B3Z assays, Ana1/B16 was seeded at a cell density of at least 1 x 10<sup>4</sup> cells per well (optimised around 5 x 10<sup>4</sup> cells per well), in 100  $\mu$ L. Medium conditions were added, such as 25 ng/mL IFN- $\gamma$  or 1  $\mu$ M SIINFEKL peptide. Aqua dest was added to the outside wells to reduce evaporation of the medium. Cells were left in the incubator for 3 to 5 hours to have time to attach to the well bottom. Subsequently, B3Z was added at a density of 3 x 10<sup>4</sup> cells per well and the cells were incubated overnight at 37 °C. The following day, the plate was spun down at 250 RCF for 5 minutes at 21 °C and supernatant was removed from all wells. The assay readout was started by adding 100  $\mu$ L Z buffer [250  $\mu$ L  $\beta$ ME, 40 mg MgCl<sub>2</sub> (Merck KGAA, Darmstadt Germany), 25  $\mu$ L nonidet P-40 (Sigma Chemical Co., St. Louis USA) and 1,76 mg CPRG (Roche, Mannheim Germany) to 20 mL PBS] and incubating for 4 hours at 37 °C, shaking. Readout was done using a 96 wells plate reader at endpoint reading, wavelength of 595 and 5 seconds of mix time.



## References

1. Moingeon P. Cancer vaccines. *Vaccine*. 2001;19(11–12):1305–26.
2. Heemskerk MHM, Hoogeboom M, Hagedoorn R, Kester MGD, Willemze R, Falkenburg JHF. Reprogramming of Virus-specific T Cells into Leukemia-reactive T Cells Using T Cell Receptor Gene Transfer. *J Exp Med* [Internet]. 2004 Apr 5 [cited 2021 Mar 17];199(7):885–94. Available from: <http://www.jem.org/cgi/doi/10.1084/jem.20031110>
3. Tye-Din JA, Cameron DJS, Daveson AJ, Day AS, Dellsperger P, Hogan C, et al. Appropriate clinical use of human leukocyte antigen typing for coeliac disease: An Australasian perspective. *Intern Med J*. 2015;45(4):441–50.
4. Gernez Y, Nowak-Węgrzyn A. Immunotherapy for Food Allergy: Are We There Yet? *J Allergy Clin Immunol Pract*. 2017 Apr 1;5(2):250–72.
5. Dong Y, Zhang S, Wu Z, Li X, Wang WL, Zhu Y, et al. Cryo-EM structures and dynamics of substrate-engaged human 26S proteasome. *Nature* [Internet]. 2019 Jan 3 [cited 2021 Mar 17];565(7737):49–55. Available from: </pmc/articles/PMC6370054/>
6. Jukič M, Grabrijan K, Kadić S, De Lera Garrido FJ, Sosič I, Gobec S, et al. Chlorocarbonylsulfonyl chloride cyclizations towards piperidin-3-yl-oxathiazol-2-ones as potential covalent inhibitors of threonine proteases. *Acta Chim Slov*. 2017;64(4):771–81.
7. Tanaka K. The proteasome: Overview of structure and functions.
8. Purcell AW, Elliott T. Molecular machinations of the MHC-I peptide loading complex. Vol. 20, *Current Opinion in Immunology*. Elsevier Current Trends; 2008. p. 75–81.
9. Fremont DH, Stura EA, Šp M, Šii PAP, Wilson IA, Kappler JW, et al. Crystal structure of an H-2Kb-ovalbumin peptide complex reveals the interplay of primary and secondary anchor positions in the major histocompatibility complex binding groove (murine major histocompatibility complex class I/allele-specific motifs/x-ray crystallography) "Present address: R ttThe atomic coordinates have been deposited in the Protein Data. Vol. 92, *Immunology*. 1995.
10. Gray1 ML, Killinger AH. *Listeria monocytogenes* and Listeric Infections. Vol. 30, *BACTERIOLOGICAL REVIEWS*. 1966.
11. Symptoms | *Listeria* | CDC [Internet]. [cited 2021 Sep 26]. Available from: <https://www.cdc.gov/listeria/symptoms.html>
12. T'dney LG, Portnoy DA. Actin Filaments and the Growth, Movement, and Spread of the Intracellular Bacterial Parasite, *Listeria monocytogenes* [Internet]. [cited 2021 Mar 22]. Available from: <http://rupress.org/jcb/article-pdf/109/4/1597/1058347/1597.pdf>
13. Liepe J, Mishto M, Textoris-Taube K, Janek K, Keller C, Henklein P, et al. The 20S Proteasome Splicing Activity Discovered by SpliceMet. De Boer RJ, editor. *PLoS Comput Biol* [Internet]. 2010 Jun 24 [cited 2021 Sep 8];6(6):e1000830. Available from: <https://dx.plos.org/10.1371/journal.pcbi.1000830>
14. Platteel ACM, Mishto M, Textoris-Taube K, Keller C, Liepe J, Busch DH, et al. CD8<sup>+</sup> T cells of *Listeria monocytogenes*-infected mice recognize both linear and spliced proteasome products. *Eur J Immunol* [Internet]. 2016 May 1 [cited 2021 Sep 8];46(5):1109–18. Available from: <https://onlinelibrary.wiley.com/doi/10.1002/eji.201545989>
15. Zhang M, Fritsche J, Roszik J, Williams LJ, Peng X, Chiu Y, et al. RNA editing derived epitopes function as cancer antigens to elicit immune responses. *Nat Commun* [Internet]. 2018 Dec 1



- [cited 2021 Jul 25];9(1):1–10. Available from: [www.nature.com/naturecommunications](http://www.nature.com/naturecommunications)
16. Chong C, Müller M, Pak HS, Harnett D, Huber F, Grun D, et al. Integrated proteogenomic deep sequencing and analytics accurately identify non-canonical peptides in tumor immunopeptidomes. *Nat Commun.* 2020;11(1).
  17. Vigneron N, Stroobant V, Chapiro J, Ooms A, Morel S, Bruggen P Van Der, et al. An Antigenic Peptide Produced by Peptide Splicing in the Proteasome Published by : American Association for the Advancement of Science Stable URL : <http://www.jstor.org/stable/3836724> Your use of the JSTOR archive indicates your acceptance of the Terms & . 2016;304(5670):587–90.
  18. Platteel ACM, Liepe J, van Eden W, Mishto M, Sijts AJAM. An Unexpected Major Role for Proteasome-Catalyzed Peptide Splicing in Generation of T Cell Epitopes: Is There Relevance for Vaccine Development? *Front Immunol [Internet]*. 2017 Nov 3 [cited 2021 Jul 17];8(NOV):1441. Available from: <http://journal.frontiersin.org/article/10.3389/fimmu.2017.01441/full>
  19. Karttunen J, Sanderson S, Shastri N. Detection of rare antigen-presenting cells by the lacZ T-cell activation assay suggests an expression cloning strategy for T-cell antigens. Vol. 89. 1992.
  20. Hashimoto M, Yamashita Y, Takemoto T. Electroporation of Cas9 protein/sgRNA into early pronuclear zygotes generates non-mosaic mutants in the mouse. *Dev Biol.* 2016 Oct 1;418(1):1–9.
  21. Sun C, Ouyang M, Cao Z, Ma S, Alqublan H, Sriranganathan N, et al. Electroporation-delivered fluorescent protein biosensors for probing molecular activities in cells without genetic encoding. *Chem Commun.* 2014;50(78):11536–9.
  22. Gräslund S, Nordlund P, Weigelt J, Martin Hallberg B, Bray J, Gileadi O, et al. Protein production and purification. Shigeyuki Yokoyama [Internet]. 2008 [cited 2021 Sep 13];18(2):135–46. Available from: <http://targetdb.pdb.org/>
  23. Platteel ACM, Liepe J, Textoris-Taube K, Keller C, Henklein P, Schalkwijk HH, et al. Multi-level Strategy for Identifying Proteasome-Catalyzed Spliced Epitopes Targeted by CD8+ T Cells during Bacterial Infection. *Cell Rep [Internet]*. 2017;20(5):1242–53. Available from: <http://dx.doi.org/10.1016/j.celrep.2017.07.026>
  24. Chen W, Carbone FR, McCluskey J. Electroporation and commercial liposomes efficiently deliver soluble protein into the MHC class I presentation pathway. Priming in vitro and in vivo for class I-restricted recognition of soluble antigen. *J Immunol Methods.* 1993 Jan 1;160(1):49–57.
  25. Ovaa Janssen H, Neefjes JJ, M Schumacher TN, Schuurman B, Linnemann C, Meiring HD, et al. Presentation by MHC Class I Molecules Rules for High-Efficiency Spliced Peptide Definition of Proteasomal Peptide Splicing Downloaded from. 2021 [cited 2021 Oct 27];27:2021. Available from: <http://www.jimmunol.org/content/195/9/4085><http://www.jimmunol.org/>
  26. Paes W, Leonov G, Partridge T, Nicastri A, Ternette N, Borrow P. Elucidation of the Signatures of Proteasome-Catalyzed Peptide Splicing. *Front Immunol [Internet]*. 2020 Sep 24 [cited 2021 Sep 26];11:2355. Available from: <https://www.frontiersin.org/articles/10.3389/fimmu.2020.563800/full>